



# Comparative Study of Different Stellar Tracks and Isochrones

Devarshi Choudhury\*, Amith Govind†, Blesson Mathew‡ and Paul K. T.§

## Abstract

With better understanding of the working physics behind the formation and evolution of stars, it has become increasingly important for observers to use an appropriate set of stellar evolutionary tracks and isochrones with respect to the objects of interest. We present a comparative study of three widely used competent stellar models – MIST, PARSEC and Siess. We analyze their input physics and the final tracks thus generated, especially focusing on the behaviour of the models during the pre-main sequence phase.

**Keywords:** Stellar Tracks, Isochrones, Astronomy, Astrophysics

## 1. Introduction

In recent years, advancement in the study of the star-formation and planet-formation processes have demanded increased observations of pre-main sequence (PMS) stars. These objects are larger and more luminous than their main-sequence counterparts, powered by gravitational contraction and deuterium fusion. This phase ends with the onset of hydrogen burning and the star arrives at the Zero Age Main Sequence (ZAMS). In order to determine mass, age and other stellar parameters of observed PMS stars, one needs to employ two very useful tools in their corresponding colour-magnitude diagram (CMD) – stellar evolutionary tracks and isochrones.

Evolutionary tracks are generated by points on a CMD that denote how any star of a particular mass would evolve, while isochrones are

---

\*Anton Pannekoek Institute for Astronomy, University of Amsterdam; [devarshi.choudhury@student.uva.nl](mailto:devarshi.choudhury@student.uva.nl)

†Department of Physics and Astronomy, University of Bonn; [s6amgovi@uni-bonn.de](mailto:s6amgovi@uni-bonn.de)

‡CHRIST (Deemed to be University); [blesson.mathew@christuniversity.in](mailto:blesson.mathew@christuniversity.in)

§CHRIST (Deemed to be University); [paul.kt@christuniversity.in](mailto:paul.kt@christuniversity.in)

plots on a CMD connecting stellar populations at constant time across all masses. With several large databases of these tracks available in literature, comparisons reveal the underlying theoretical discrepancies and uncertainties associated with various derived parameters. Tracks produced by various groups differ in their code because of the many prescriptions used to describe the physical processes driving the evolution. The most important processes that affect the morphology and position of the tracks are the adopted chemical composition and distribution, sources of opacities, convective models and its related properties, the initial mass function (IMF), and the star formation rate (SFR).

In this paper, we present a comparison of the processes involved in the stellar models of MESA Isochrones and Stellar Tracks (MIST) [10, 13], PARSEC stellar tracks and isochrones [5], and tracks and isochrones by Siess [39, 40]. These models are also accessible through interfaces over the internet. The input physics behind these models are compared in Section 2. Section 3 describes the different tracks generated. We provide our concluding remarks in Section 4.

## 2. Input Physics

### 2.1 Abundances

For decades, concerted efforts have been made for the accurate determination of solar abundances. Models of Siess have accounted for partially ionised plasma, and performed computations at four different metallicities ( $Z = 0.01 - 0.04$ ). Abundances of heavy elements have been taken from [3]. They have included non-ideal effects of Coulomb shielding for all elements and pressure ionization for H, He, C, N and O, except for  $H^-$ . Other species are considered to be neutral or completely ionized, either of which does not affect the structure and evolution of low mass ( $M < 3M_{\odot}$ ) PMS stars. For more massive stars, models assuming total ionizations for heavy elements have a moderately shallower convective region initially, which disappears upon the arrival on ZAMS.

PARSEC models consider a reference solar distribution of metals consisting of 90 elements from Li to U, the abundances of which have been taken from Grevesse *et al.* [19] and Caffau *et al.* [7], with a few elements assigned negligible abundances. Based on the abundance compilation, they compute models over a wider metallicity range ( $Z = 0.0005 - 0.07$ ). They derived the present-day Sun's metallicity  $Z_{\odot} = 0.01524$ , and assigned fractional abundances relative to the total solar metallicity i.e.  $X_{i,\odot}/Z_{\odot}$ , for elements heavier than  ${}^4\text{He}$ . Besides the solar distribution of elements, other distributions representative of galaxies with particular chemical evolution histories, e.g. Magel-

lanic Clouds, have also been considered.

MIST models adopted protostellar abundances from [4] as the reference scale for all metallicities ( $-2.0 \leq [Z/H] \leq 0.5$ ). A grid considering the evolution from the PMS phase to the end of core He burning for  $-4.0 \leq [Z/H] \leq -2.0$  is also provided.  $[Z/H]$  is computed with respect to  $Z_{\odot} = 0.0142$ . They use [4] as the reference scale since it provides revised abundances for C, N, O and Ne. This revision accounts for improved atomic and molecular linelists and modeling techniques utilizing 3D non-local thermodynamic equilibrium (NLTE) hydrodynamics. Primordial He abundance is also accounted for as  $Y_p = 0.249$ , adopted from Planck Collaboration project [33].

## 2.2 Opacities

At high-temperature ( $>8000\text{K}$ ), tracks by Siess make use of the radiative opacities provided by the Opacity Project At Livermore (OPAL) [22]. Low-temperature radiative opacities were adopted from Alexander and Ferguson [2] tables, which are especially suited for cool sub-photospheric regions and red sub-giant atmospheres. Conductive opacities were adopted from Iben [21]. Tables for non-relativistic electrons were imported from Itoh *et al.* [23] and Mitake *et al.* [31], and for relativistic electrons from Itoh *et al.* [24] Calculation by Raikh and Iakovlev [35] for solid plasmas are also adopted.

The models by PARSEC make use of pre-computed static tables of Rosseland mean opacities to describe the absorption properties of gaseous matter. At higher temperatures ( $4.2 \leq \log(T/\text{K}) \leq 8.7$ ), opacity tables by OPAL have been used and at lower temperatures ( $3.2 \leq \log(T/\text{K}) \leq 4.1$ ) they make use of the AESOPUS tool [28], which solves for matter in a gaseous state for 800 chemical species. These account for the different continuum and discrete sources. Conductive opacities have been accounted for as well [25].

For high-temperature regimes ( $\log T \geq 4$ ), MIST models also make use of tables by OPAL and the Opacity Project (OP) [38]. For low-temperatures, users get to choose between Ferguson *et al.* [14] or Freedman *et al.* [15] Ammonia opacity have also been considered [43] along with the pressure-induced opacity for  $\text{H}_2$  from Frommhold *et al.* [16] and electron conduction opacity tables based on Cassusu *et al.* [8] and Paxton *et al.* [32]

## 2.3 Equation of State

The equation of state (EOS) in Siess is analytic and takes into consideration the effects of pressure ionization, partially degenerate matter and Coulomb interactions. They account for the electrostatic corrections following statistical models, and also correct for the continuum depression in ionization potentials. The model assumes a local ther-

modynamic equilibrium on which Saha equations can be applied. The plasma is accounted for by three components—electrons, photons and ions, which are coupled through the processes of photo-ionization and photo-dissociation.

The PARSEC accounts for the contributions of several elements in its EOS calculations. Thermodynamic quantities such as mass, density, mean molecular weight, entropy, specific heat and their derivatives are accounted for each value of  $Z$ , over sufficiently wide temperature and pressure ranges. They have arranged two sets of tables classified as ‘H-rich’ and ‘H-free’. The H-rich set consist of 10 tables with unique H abundances and the H-free set contains 31 tables describing the He-burning regions.

The EOS tables in MESA are based on SCVH tables [37] at lower temperatures and densities, and on EOS tables by OPAL [36] at higher regimes. At higher metallicities, tables are based on MacDonald EOS tables [27] since they allow for partially ionized species. At temperature and density scales beyond the scope of the above mentioned tables, they make use of HELM and PC tables [34] which assume full ionization. MESA EOS also considers plasma interaction and application of Coulomb coupling parameter. They even cover the the late stages of white dwarf cooling during which the ions in the core crystallize.

#### 2.4 Convective Zones

The structure of convective zones in Siess models have been computed using the Mixing-Length Theory (MLT) as per Kippenhahn [26] prescription. Overshoot has only been computed for the grid with solar composition ( $Z = 0.02$ ). Once nuclear transformations take place inside convective regions, instantaneous mixing is assumed. For a solar mixture, stars with masses  $\leq 0.4M_{\odot}$  are fully convective throughout their evolution. Stars with masses  $\geq 1.1M_{\odot}$  do not burn more than 30% of their initial  ${}^6\text{Li}$  when mixing mechanisms are absent. When a moderate overshooting is considered, stars with a convective core exhibit increased duration on main sequence (MS), and results in additional Li burning in the PMS phase.

The extension of convective boundary of the core in PARSEC is computed taking into account a moderate amount of overshooting from the central convective region [6]. In order to account for the transition of MS models with radiative and convective cores, a variable overshoot parameter is employed to describe the overshoot development. A smooth transition of properties between models with radiative and convective cores is ensured by a linearly increasing overshooting efficiency with increasing mass. The region of overshoot is considered to be radiative instead of adiabatic, which results in an overall larger mixed core. The base of the convective envelope may

generate a sizable overshoot region. To account for such a possibility, the temperature gradient of this region is kept equal to the radiative one.

Models by MIST compute convective heat flux by solving MLT cubic equations of Henyey *et al.* [20] to obtain their temperature gradients. The convective mixing of elements is performed as a diffusive process that is time-dependent in nature. MLT formalisms also are used to compute the corresponding diffusion coefficient which is subject to modification by overshoot mixing. This mixing with modest overshoot efficiencies is performed as per two prescriptions – step overshoot, and decay of velocity fields and eventual disintegration of convective elements in the overshoot region by the diffusion process. The strength of convective overshoot is calibrated purely empirically.

### 2.5 Nuclear Reaction Rates

Nuclear reaction rates of Siess have been adopted from Caughlan and Fowler [9]. The weak and intermediate screening factors have been accounted for by applying formalisms found in Graboske *et al.* [18]. Using the Wagoner [42] algorithm, nuclide abundances have been computed.

Nuclear network of PARSEC consists of p-p chains, CNO tri-cycle, Ne-Na and Mg-Al chains, and  $\alpha$ -capture reactions. The reaction rates of 26 chemical species have been taken from the JINA REACLIB database [11] whose abundances are solved for by the network. Dewitt *et al.* [12] and Graboske *et al.* [18] provide the electron screening factors, and the abundances are evaluated using a semi-implicit extrapolation scheme described in [29].

MIST models, like PARSEC also adopt the reaction rates from JINA REACLIB database for p-p chains, CNO cycles, the Ne-Na and Mg-Al chains, C/O burning and  $\alpha$ -capture processes. Triple- $\alpha$  process rates have been imported from Fynbo *et al.* [17] The nuclear network tracks solve for the abundance of 52 species. Electron screening for all regimes have been computed by extending Graboske *et al.* [18] with that of Alastuey and Jancovici [1].

### 2.6 Other Factors

Apart from the above mentioned major physical processes involved behind these models, there are also multiple other factors that have been accounted for by different groups. We provide a brief comparison on some of them in this section.

Atmospheres have been computed for all the models. Siess integrates stellar structure to a very low optical depth ( $\tau = 0.005$ ) in the atmosphere, performing an analytic fit of  $T(\tau)$  as a function of  $T_{eff}$ ,  $g_{eff}$  and  $Z$ . PARSEC has adopted a plane-parallel grey model for their

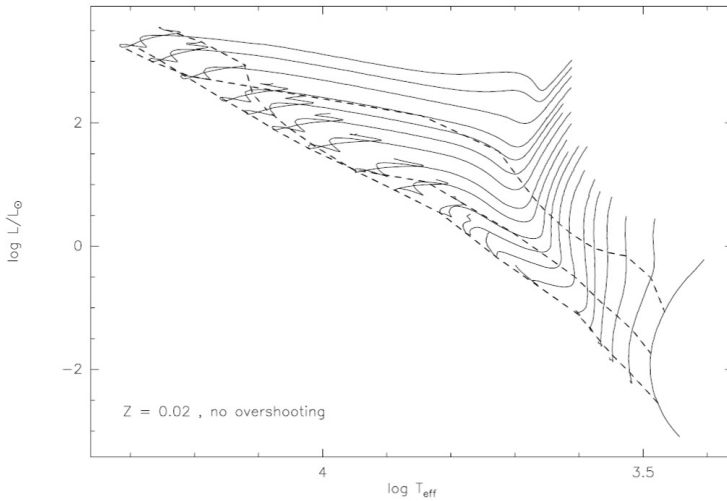


**Figure 1.** Evolutionary tracks from 7.0 to 0.1  $M_{\odot}$  for solar metallicity with Isochrones (dashed lines) corresponding to  $10^6$ ,  $10^7$ ,  $10^8$  years [40]

atmosphere, where a modified Eddington approximation for radiative transport accounts for the temperature stratification. Models of MIST make use of analytic approximations as well as tables of atmospheric structure for various mass ranges.

The effects of microscopic diffusion and gravitational settling of elements have been considered by both PARSEC and MIST based on diffusion coefficient calculations following [41]. In both cases, diffusion is not implemented for stars that develop a persistent convective core. Energy losses by electron and plasma neutrinos are also accounted for only in the models of PARSEC and MIST. These models also consider for breathing pulses and semiconvection following the core He burning (CHeB) phase. The process of mass loss has not been accounted for in PARSEC and Siess, but is implemented in MIST based on observational and theoretical prescriptions. They are also the only models accounting for the effects of rotation.

### 3. Model Outputs

Models by Siess include 29 mass tracks across the range 0.1 – 7.0  $M_{\odot}$ . Figure 1 shows these tracks along with certain isochrones. Due to composition differences, ZAMS locations by Siess are slightly different from previous works in literature. Comparison of the observational ZAMS derived by Mermilliod [30] with its predicted location based on Siess reveal good agreement (Figure 2). For low mass ob-

jects the model requires a better treatment of electrostatic corrections. Comparison of their isochrones with previous works again shows similarity down to  $0.6 M_{\odot}$  however. Age determination is uncertain below  $10^6$  yr.

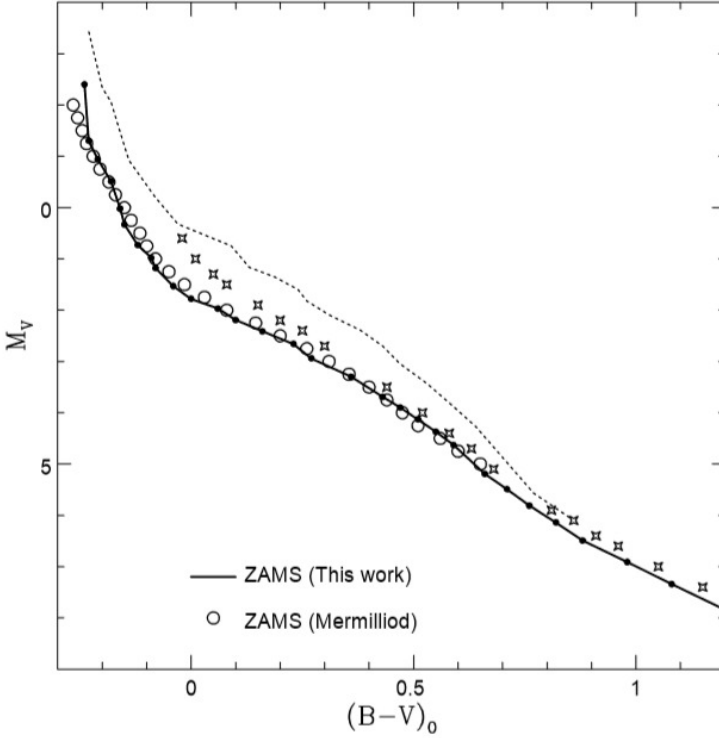


**Figure 2.** Observed vs predicted location of ZAMS. TAMS is represented by dashed lines, and crosses represent Schmidt-Kaler compilation of MS location [39]

PARSEC computes tracks (Figure 3) for stars with initial masses between  $0.1 - 12 M_{\odot}$  and allows for a smooth transition from low to intermediate to high-mass stars. PMS lifetimes are treated as a function of stellar mass. After PMS evolution the model is no longer homogeneous due to alterations in the abundances of certain light elements. These result in the formation of loops that are dependent on the initial mass and chemical composition. The tracks are divided into suitable homogeneous evolutionary phases and then used to compute isochrones by interpolating along missing stellar tracks (Figure 4). PARSEC isochrones do not cover the TP-AGB or the post-AGB phases.

MIST evolutionary tracks (Figure 5) span the mass range  $0.1 - 300 M_{\odot}$ . They compute for evolution from the PMS phase to the end of hydrogen burning, WD cooling phase, or the end of carbon burning,

that is dependent on the initial mass and metallicity of the star.

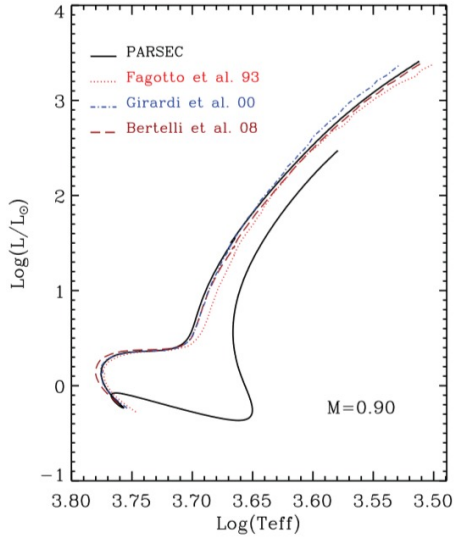


**Figure 3.** PARSEC evolutionary track with  $Z=0.008$  compared with other databases with slightly varying He content[10]

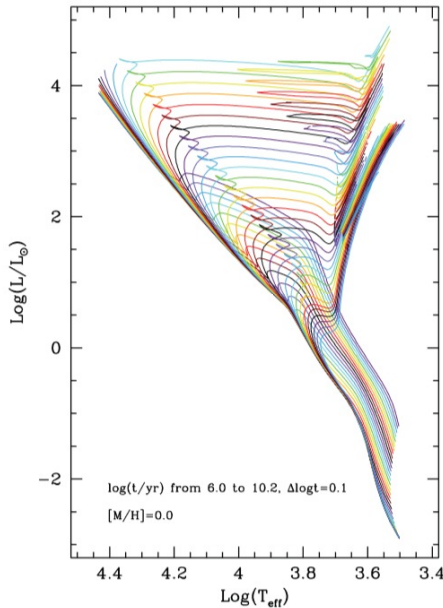


**Figure 4:** Sequence of solar-metallicity isochrones for ages  $\log(t/\text{yr})=6-10.2$ [10]



Stars in the MS appear more luminous when rotation is considered which promotes core growth. Isochrones are generated by defining two sets of equivalent evolutionary phases (EEPs). Primary EEPs are based on physically motivated phases in the track while secondary EEPs provide a uniform spacing between the primary EEPs.

#### 4. Conclusion

The selection of evolutionary tracks and isochrones is entirely dependent on the stellar population of interest and one must be very cautious when choosing a particular model in order to account for the relevant mechanisms affecting said models. After comparing the evolutionary models and isochrones of Siess, PARSEC and MIST, and having highlighted their major characteristics, we arrive at the following conclusion:

- Although models by Siess make use of older generation of various databases and tables for computing purposes, they are still appropriate for use, and are especially apt if the objects of interest are in the very low mass range. They are also fairly suitable when considering grids of PMS tracks.
- PARSEC models are well-suited for the study of stellar populations over the provided mass range in globular clusters and quiescent galaxies, especially for lower mass candidates. Their isochrones also vary on the lower MS due to empirically calibrated boundary conditions made to match the observed mass-radius relations for cool dwarfs.
- Models by MIST make use of the most up-to-date databases for their computations, accounting for many more factors and inputs than the other models. They are particularly useful for generating tracks that continuously follow the evolution from the He ignition in the degenerate core to the CHeB through a series of He flashes.

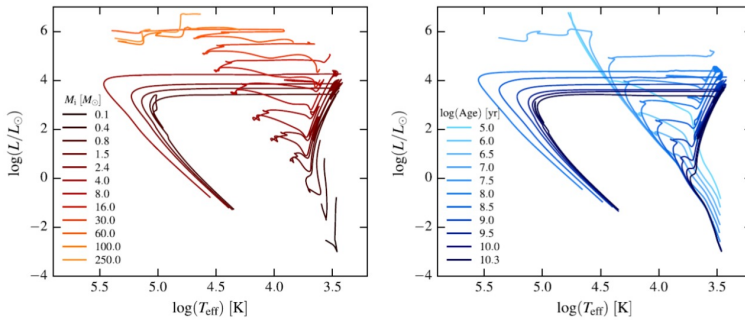


**Figure 5.** Tracks and isochrones by MIST [10]. Solar metallicity grid of evolutionary tracks (left) and isochrones covering range of stellar masses, ages and evolutionary phases (right)

## Acknowledgments

We would like to thank the teams behind MIST and PARSEC, and Lionel Siess of the Institute of Astronomy and Astrophysics at the Université Libre de Bruxelles for providing freely available web interfaces that generate evolutionary tracks and isochrones (MIST[44], PARSEC [45] and Siess [46]).

## References

- [1] A. Alastuey and B. Jancovici, “Nuclear reaction rate enhancement in dense stellar matter,” *The Astrophysical Journal*, vol. 226, pp. 1034–1040, Dec. 1978.
- [2] D. R. Alexander and J. W. Ferguson, “Low-temperature Rosseland opacities,” *The Astrophysical Journal*, vol. 437, pp. 879–891, Dec. 1994.
- [3] E. Anders and N. Grevesse, “Abundances of the elements - Meteoritic and solar,” *Geochimica et Cosmochimica Acta*, vol. 53, pp. 197–214, Jan. 1989.
- [4] M. Asplund, N. Grevesse, A. J. Sauval, and P. Scott, “The Chemical Composition of the Sun,” *Annual Review of Astronomy and Astrophysics*, vol. 47, pp. 481–522, Sep. 2009.
- [5] A. Bressan, P. Marigo, L. Girardi, B. Salasnich, C. Dal Cero, S. Rubele and A. Nanni, “PARSEC: stellar tracks and isochrones with the PADova and TRIeste Stellar Evolution Code,” *Monthly Notices of the Royal Astronomical Society*, vol. 427, pp. 127–145, Nov. 2012.
- [6] A. G. Bressan, C. Chiosi and G. Bertelli, “Mass loss and overshooting in massive stars,” *Astronomy and Astrophysics*, vol. 102, pp. 25–30, Sep. 1981.
- [7] E. Caffau, H.-G. Ludwig, M. Steffen, B. Freytag and P. Bonifacio, “Solar Chemical Abundances Determined with a CO5BOLD 3D Model Atmosphere,” *Solar Physics*, vol. 268, pp. 255–269, Feb. 2011.
- [8] S. Cassisi, A. Y. Potekhin, A. Pietrinferni, M. Catelan and M. Salaris, “Updated Electron-Conduction Opacities: The Impact on Low-Mass Stellar Models,” *The Astrophysical Journal*, vol. 661, pp. 1094–1104, Jun. 2007.

- [9] G. R. Caughlan and W. A. Fowler, “Thermonuclear Reaction Rates V,” *Atomic Data and Nuclear Data Tables*, vol. 40, p. 283, 1988.
- [10] J. Choi, A. Dotter, C. Conroy, M. Cantiello, B. Paxton and B. D. Johnson, “Mesa Isochrones and Stellar Tracks (MIST). I. Solar-scaled Models,” *The Astrophysical Journal*, vol. 823, p. 102, Jun. 2016.
- [11] R. H. Cyburt, A. M. Amthor, R. Ferguson, Z. Meisel, K. Smith, S. Warren, A. Heger, R. D. Hoffman, T. Rauscher, A. Sakharuk, H. Schatz, F. K. Thielemann and M. Wiescher, “The JINA REACLIB Database: Its Recent Updates and Impact on Type-I X-ray Bursts,” *Astrophysical Journal Supplement*, vol. 189, pp. 240–252, Jul. 2010.
- [12] H. E. Dewitt, H. C. Graboske and M. S. Cooper, “Screening Factors for Nuclear Reactions. I. General Theory,” *The Astrophysical Journal*, vol. 181, pp. 439–456, Apr. 1973.
- [13] A. Dotter, “MESA Isochrones and Stellar Tracks (MIST) 0: Methods for the Construction of Stellar Isochrones,” *The Astrophysical Journal Supplement Series*, vol. 222, p. 8, Jan. 2016.
- [14] J. W. Ferguson, D. R. Alexander, F. Allard, T. Barman, J. G. Bodnarik, P. H. Hauschildt, A. Heffner-Wong and A. Tamanai, “Low-Temperature Opacities,” *The Astrophysical Journal*, vol. 623, pp. 585–596, Apr. 2005.
- [15] R. S. Freedman, M. S. Marley, and K. Lodders, “Line and Mean Opacities for Ultracool Dwarfs and Extrasolar Planets,” *The Astrophysical Journal Supplement Series*, vol. 174, pp. 504–513, Feb. 2008.
- [16] L. Frommhold, M. Abel, F. Wang, X. Li and K. L. C. Hunt, “Collision-induced absorption at temperatures of thousands of kelvin, from first principles, for astrophysical applications,” in *American Institute of Physics Conference Series*, ser. American Institute of Physics Conference Series, J. Lewis and A. Predoi-Cross, Eds., vol. 1290, Oct. 2010, pp. 219–230.
- [17] H. O. U. Fynbo, C. A. Diget, U. C. Bergmann, M. J. G. Borge, J. Cederkäll, P. Dendooven, L. M. Fraile, S. Franchoo, V. N. Fedosseev, B. R. Fulton, W. Huang, J. Huikari, H. B. Jeppesen, A. S. Jokinen, P. Jones, B. Jonson, U. Köster, K. Langanke, M. Meister, T. Nilsson, G. Nyman, Y. Prezado, K. Riisager, S. Rinta-Antila, O. Tengblad, M. Turrion, Y. Wang, L. Weissman, K. Wilhelmsen, J. Äystö and ISOLDE Collaboration, “Revised rates for the stellar triple- $\alpha$  process from measurement of  $^{12}\text{C}$  nuclear resonances,” *Nature*, vol. 433, pp. 136–139, Jan. 2005.
- [18] H. C. Graboske, H. E. Dewitt, A. S. Grossman and M. S. Cooper, “Screening Factors for Nuclear Reactions. II. Intermediate Screen-Ing and Astrophysical Applications,” *The Astrophysical Journal*, vol. 181, pp. 457–474, Apr. 1973.
- [19] N. Grevesse and A. J. Sauval, “Standard Solar Composition,” *Space Science Reviews*, vol. 85, pp. 161–174, May 1998.
- [20] L. Henyey, M. S. Vardya and P. Bodenheimer, “Studies in Stellar Evolution. III. The Calculation of Model Envelopes,” *The Astrophysical Journal*, vol. 142, p. 841, Oct. 1965.
- [21] I. Iben, Jr., “Thermal pulses; p-capture, alpha-capture, s-process nucleosynthesis; and convective mixing in a star of intermediate mass,” *The Astrophysical Journal*, vol. 196, pp. 525–547, Mar. 1975.
- [22] C. A. Iglesias and F. J. Rogers, “Updated Opal Opacities,” *The Astrophysical Journal*, vol. 464, p. 943, Jun. 1996.
- [23] N. Itoh, S. Mitake, H. Iyetomi and S. Ichimaru, “Electrical and thermal conductivities of dense matter in the liquid metal phase. I - High-temperature results,” *The Astrophysical Journal*, vol. 273, pp. 774–782, Oct. 1983.

- [24] N. Itoh, Y. Kohyama, N. Matsumoto and M. Seki, "Electrical and thermal conductivities of dense matter in the crystalline lattice phase," *The Astrophysical Journal*, vol. 285, pp. 758–765, Oct. 1984.
- [25] N. Itoh, S. Uchida, Y. Sakamoto, Y. Kohyama and S. Nozawa, "The Second Born Corrections to the Electrical and Thermal Conductivities of Dense Matter in the Liquid Metal Phase," *The Astrophysical Journal*, vol. 677, pp. 495–502, Apr. 2008.
- [26] R. Kippenhahn, H.-C. Thomas and A. Weigert, "Entwicklung in engen Doppeltsternsystemen V. Thermal Pulses in the White Dwarf Component of a Binary System," *Zeitschrift für Astrophysik*, vol. 69, p. 265, 1968.
- [27] J. MacDonald and D. J. Mullan, "Precision modelling of M dwarf stars: the magnetic components of CM Draconis," *Monthly Notices of the Royal Astronomical Society*, vol. 421, pp. 3084–3101, Apr. 2012.
- [28] P. Marigo and B. Aringer, "Low-temperature gas opacity. ÆSOPUS: a versatile and quick computational tool," *Astronomy and Astrophysics*, vol. 508, pp. 1539–1569, Dec. 2009.
- [29] P. Marigo, L. Girardi, C. Chiosi and P. R. Wood, "Zero-metallicity stars. I. Evolution at constant mass," *Astronomy and Astrophysics*, vol. 371, pp. 152–173, May 2001.
- [30] J. C. Mermilliod, "Comparative studies of young open clusters. III - Empirical isochronous curves and the zero age main sequence," *Astronomy and Astrophysics*, vol. 97, pp. 235–244, Apr. 1981.
- [31] S. Mitake, S. Ichimaru and N. Itoh, "Electrical and thermal conductivities of dense matter in the liquid metal phase. II - Low-temperature quantum corrections," *The Astrophysical Journal*, vol. 277, pp. 375–378, Feb. 1984.
- [32] B. Paxton, M. Cantiello, P. Arras, L. Bildsten, E. F. Brown, A. Dotter, C. Mankovich, M. H. Montgomery, D. Stello, F. X. Timmes and R. Townsend, "Modules for Experiments in Stellar Astrophysics (MESA): Planets, Oscillations, Rotation, and Massive Stars," *Astrophysical Journal Supplement*, vol. 208, p. 4, Sep. 2013.
- [33] Planck Collaboration, P. A. R. Ade, N. Aghanim, M. Arnaud, M. Ashdown, J. Aumont, C. Baccigalupi, A. J. Banday, R. B. Barreiro, J. G. Bartlett *et al.*, "Planck 2015 results. XIII. Cosmological parameters," *Astronomy and Astrophysics*, vol. 594, p. A13, Sep. 2016.
- [34] A. Y. Potekhin and G. Chabrier, "Thermodynamic Functions of Dense Plasmas: Analytic Approximations for Astrophysical Applications," *Contributions to Plasma Physics*, vol. 50, pp. 82–87, Jan. 2010.
- [35] M. E. Raikh and D. G. Iakovlev, "Thermal and electrical conductivities of crystals in neutron stars and degenerate dwarfs," *Astrophysics and Space Science*, vol. 87, pp. 193–203, Oct. 1982.
- [36] F. J. Rogers and A. Nayfonov, "Updated and Expanded OPAL Equation-of-State Tables: Implications for Helioseismology," *The Astrophysical Journal*, vol. 576, pp. 1064–1074, Sep. 2002.
- [37] D. Saumon, G. Chabrier and H. M. van Horn, "An Equation of State for Low-Mass Stars and Giant Planets," *Astrophysical Journal Supplement*, vol. 99, p. 713, Aug. 1995.
- [38] M. J. Seaton, "Opacity Project data on CD for mean opacities and radiative accelerations," *Monthly Notices of the Royal Astronomical Society*, vol. 362, pp. L1–L3, Sep. 2005.
- [39] L. Siess, M. Forestini, and C. Dougados, "Synthetic Hertzsprung-Russell diagrams of open clusters," *Astronomy and Astrophysics*, vol. 324, pp. 556–565, Aug. 1997.

- [40] L. Siess, E. Dufour and M. Forestini, “An internet server for pre-main sequence tracks of low- and intermediate-mass stars,” *Astronomy and Astrophysics*, vol. 358, pp. 593–599, Jun. 2000.
- [41] A. A. Thoul, J. N. Bahcall and A. Loeb, “Element diffusion in the solar interior,” *The Astrophysical Journal*, vol. 421, pp. 828–842, Feb. 1994.
- [42] R. V. Wagoner, “Synthesis of the Elements Within Objects Exploding from Very High Temperatures,” *Astrophysical Journal Supplement*, vol. 18, p. 247, Jun. 1969.
- [43] S. N. Yurchenko, R. J. Barber and J. Tennyson, “A variationally computed line list for hot NH<sub>3</sub>,” *Monthly Notices of the Royal Astronomical Society*, vol. 413, pp. 1828–1834, May 2011.
- [44] <http://waps.cfa.harvard.edu/MIST/index.html>
- [45] <http://stev.oapd.inaf.it/cgi-bin/cmd>
- [46] <http://www.astro.ulb.ac.be/siess/pmwiki/pmwiki.php/Site/WWWTools>